Low-energy excitations in bosonic quantum quasicrystals

A. Mendoza-Coto, M. Bonifacio, Francesco Piazza

Angaben zur Veröffentlichung / Publication details:

Mendoza-Coto, A., M. Bonifacio, and Francesco Piazza. 2025. "Low-energy excitations in bosonic quantum quasicrystals." Physical Review Letters 134 (13): 136003. https://doi.org/10.1103/physrevlett.134.136003.

Featured in Physics

Low-Energy Excitations in Bosonic Quantum Quasicrystals

A. Mendoza-Coto,[1,2,*] M. Bonifacio,[2] and F. Piazza[2,3]

[1]Departamento de Física, Universidade Federal de Santa Catarina, 88040-900 Florianópolis, Brazil
[2]Max Planck Institute for the Physics of Complex Systems, Nöthnitzer Straße 38, 01187 Dresden, Germany
[3]Theoretical Physics III, Center for Electronic Correlations and Magnetism, Institute of Physics, University of Augsburg, 86135 Augsburg, Germany

(Received 3 August 2024; accepted 11 February 2025; published 2 April 2025)

We present the first principles construction of the low energy effective action for bosonic self-organized quantum quasicrystals. Our generalized elasticity approach retains the appropriate number of phase and corresponding conjugate density degrees of freedom required for a proper description of the gapless modes. For the dodecagonal and decagonal quasicrystal structures we obtain collective longitudinal and transverse excitations with an isotropic speed of sound. Meanwhile, for the octagonal structure, the coupling between phononic and phasonic degrees of freedom leads in turn to hybridization of the latter with the condensate sound mode, producing collective excitations with a longitudinal and transverse component and an anisotropic speed of sound. Finally, we discuss the fate of each excitation mode at the low and high density phase transitions limiting the quantum quasicrystal phase.

DOI: 10.1103/PhysRevLett.134.136003

Introduction—Quasicrystals (QCs) are an exotic state of matter where crystalline and disordered behavior meet. They retain long range orientational order but lack any discrete translational invariance [1–3]. Although they were initially discovered in metallic alloys [4,5], it is known today that this kind of exotic state can be stabilized in many different contexts [6–10], as long as an appropriate effective competition between two or more characteristic length scales is present in the system [11–14]. One of the most intriguing versions of quasi crystalline systems are the so-called quantum quasicrystals (QQCs) [14–20], which appear as ground states of quantum many-body Hamiltonians. The stabilization of such quasicrystaline phases have been predicted in systems like dipolar bosons with spin-orbit interactions [15], ultracold bosonic gases in quasiperiodic optical traps [18–20] (in this particular case even direct experimental observations of such phases are available [21–23]), and more recently, self-organized quasicrystals in Bose-Einstein condensates produced by cavity mediated interactions [16,24,25]. Moreover, the recent developments with twisted bilayer graphene (TBG) have opened a new route to the realization of QQCs in solid state systems [26,27].

In this Letter, we present the first principles construction of the low energy elastic theory of bosonic quantum quasicrystals, having supersolids as a particular case. Our calculations maintain full connection with the microscopic properties of the system, allowing us to make qualitative and quantitative predictions regarding the hybridization of the low momentum gapless energy modes, the corresponding propagation speed, and the behavior of these excitations at the phase boundaries of the quasicrystal phase. Furthermore, the developed method, being constructed from the microscopic action of the system, gives access to a wide range of thermodynamic properties and it serves as a systematic tool for calculating observables beyond the mean field level in a large variety of situations [28–36]. As particular examples we consider the three most relevant quasiperiodic structures in two dimensions: the octagonal, the decagonal, and the dodecagonal quasicrystals. To our knowledge, this is the first microscopic elastic theory of bosonic QQCs able to corroborate the symmetry arguments regarding the existence of five gapless excitation modes for these systems [37,38]. Our results show that the hybridization process between phonons, phasons, and the longitudinal condensate sound mode qualitatively depends on the kind of quasicrystal structure.

Model and method—We consider a 2D bosonic gas at zero temperature, interacting through an isotropic nonlocal two-body interaction of the form $Uv(r)$, where U represents a dimensionless parameter characterizing the intensity of the nonlocal interaction with respect to the kinetic energy. The nature of the two-body interaction between particles is such that the system hosts a quasicrystalline pattern at high enough particle densities in the ground state.

*Contact author: alejandro.mendoza@ufsc.br

As discussed in the literature [14,17,39], the key ingredient for the stabilization of such phases is the presence of competing minima in the interaction potential $\hat{v}(k)$. In dimensionless units, the path-integral formulation of the grand canonical partition function of the system $\mathcal{Z} = \int D\phi D\phi^* e^{-S[\phi,\phi^*]}$ [40] is characterized by the action (see [41] for a Hamiltonian formulation)

$$S[\phi,\phi^*] = \int_0^\infty d\tau \int d^2x \phi(\mathbf{x},\tau)^* \left(\partial_\tau - \frac{1}{2}\nabla^2 - \mu + \frac{U}{2}\int d^2x' v(\mathbf{x}-\mathbf{x}')|\phi(\mathbf{x}',\tau)|^2 \right) \phi(\mathbf{x},\tau). \quad (1)$$

To access the low energy properties of the system we should allow long-wavelength fluctuations of the global phase, as well as of the phase of the modulated pattern of the quasicrystal ground-state wave function which can be expanded in a Fourier basis as $\phi_0(\mathbf{x}) = \sqrt{\rho}\sum_{\mathbf{n}} c_{\mathbf{n}} \exp(i\mathbf{G}_{\mathbf{n}}\cdot\mathbf{x})$. Here ρ stands for the average particle density of the system and $c_{\mathbf{n}}$ and $\mathbf{G}_{\mathbf{n}}$ corresponds to the Fourier amplitudes and wave vectors of the pattern, respectively. We thus propose a perturbed ground state wave function of the form

$$\begin{aligned}\phi(\mathbf{x},\tau) = {} & \sqrt{\rho} c_0 \sqrt{1+\frac{\delta n_0(\mathbf{x},\tau)}{\rho c_0^2}} \exp(i\theta(\mathbf{x},\tau)) \\ & + \sum_{\mathbf{n}\neq 0} \sqrt{\rho}\, c_{\mathbf{n}} \sqrt{1+\frac{\mathbf{G}_{\mathbf{n}}\cdot\mathbf{\Pi}(\mathbf{x},\tau)}{Z} + \frac{\mathbf{G}_{\mathbf{n},\perp}\cdot\mathbf{\Pi}_\perp(\mathbf{x},\tau)}{Z_\perp}} \\ & \exp\left(i\mathbf{G}_{\mathbf{n}}\cdot\mathbf{x} + i\mathbf{G}_{\mathbf{n}}\cdot\mathbf{u}(\mathbf{x},\tau) + i\mathbf{G}_{\mathbf{n},\perp}\cdot\mathbf{w}(\mathbf{x},\tau) + i\theta(\mathbf{x},\tau)\right), \end{aligned} \quad (2)$$

where the fluctuation fields $\mathbf{u}(\mathbf{x},\tau)$ and $\mathbf{w}(\mathbf{x},\tau)$ represent the phonon and phason fields introduced as in the classical case [3,42–44]. Moreover, due to the quantum nature of the system we also have to admit fluctuations in the canonical-conjugate density fields associated to these phase variables, analogously to what was proposed by Pretko *et al.* [41] for supersolids. Accordingly, we have included the fields $\mathbf{\Pi}(\mathbf{x},\tau)$ and $\mathbf{\Pi}_\perp(\mathbf{x},\tau)$ as conjugate to $\mathbf{u}(\mathbf{x},\tau)$ and $\mathbf{w}(\mathbf{x},\tau)$, respectively. Finally, we added the overall phase fluctuation field $\theta(\mathbf{x},\tau)$ of the wave function and its canonically conjugate zero momentum density fluctuation $\delta n_0(\mathbf{x},\tau)$. It is understood that all fluctuation fields are slowly varying functions in space and imaginary time, with zero mean over the size of the system and, as expected, in the absence of fluctuations our ansatz for $\phi(\mathbf{x},\tau)$ reduces to the ground state wave function $\phi_0(\mathbf{x})$. Furthermore, the set of vectors $\{\mathbf{G}_{\mathbf{n},\perp}\}$ is constructed from a permutation of the set $\{\mathbf{G}_{\mathbf{n}}\}$, such that the extended basis $\tilde{\mathbf{G}}_{\mathbf{n}} = \mathbf{G}_{\mathbf{n}} \oplus \mathbf{G}_{\mathbf{n},\perp}$ is orthogonal in the sense $\sum_{\mathbf{n}} \tilde{\mathbf{G}}_{\mathbf{n},\alpha}\tilde{\mathbf{G}}_{\mathbf{n},\beta} \propto \delta_{\alpha,\beta}$ [3,42–44]. The ansatz considered in Eq. (2) corresponds to the most general form of $\phi(\mathbf{x},\tau)$ recovering the ground state wave function in the absence of fluctuations and preserving the symmetry properties of the action for a quasicrystal structure.

It is simple to show that the proposed ansatz satisfies the normalization condition of the boson field $\int_A d^2x\langle|\phi(\mathbf{x},\tau)|^2\rangle = N = \rho A$, as long as $\sum_{\mathbf{n}} c_{\mathbf{n}}^2 = 1$. The expectation value of an observable $\langle O\rangle = \langle\phi|O|\phi\rangle = \int_A d^2x\phi^*(\mathbf{x},t)O\phi(\mathbf{x},t)$ within our path-integral formalism is calculated as $\langle O\rangle = Z^{-1}\int D\phi D\phi^* O \exp(-S[\phi,\phi^*])$. The normalization constraint allows the calculation of the chemical potential μ for a system with a given particle density ρ. Lastly, the free parameters Z and $Z_\perp$ in Eq. (2)are chosen to enforce the expected relation between canonically conjugate fields in the low energy effective action of the system [45]. By replacing the ansatz for $\phi(\mathbf{x},\tau)$ in Eq. (1) and expanding up to quadratic order in the fluctuation fields we obtain the following long-wavelength effective action:

$$\begin{aligned}\delta S = {} & \int d\tau d^2x (i\delta n_0(\mathbf{x},\tau)\partial_\tau\theta(\mathbf{x},\tau) + i\mathbf{\Pi}(\mathbf{x},\tau)\cdot\partial_\tau\mathbf{u}(\mathbf{x},\tau) \\ & + i\mathbf{\Pi}_\perp(\mathbf{x},\tau)\cdot\partial_\tau\mathbf{w}(\mathbf{x},\tau)) + \int d\tau d^2x \frac{1}{2}[\rho(\boldsymbol{\nabla}\theta)^2 \\ & + \gamma_0\delta n_0(\mathbf{x},\tau)^2 + \gamma\mathbf{\Pi}(\mathbf{x},\tau)^2 + \gamma_\perp\mathbf{\Pi}_\perp(\mathbf{x},\tau)^2 \\ & + 2\mathbf{\Pi}\cdot\boldsymbol{\nabla}\theta + \mathbf{E}^T\tilde{C}\mathbf{E}], \end{aligned} \quad (3)$$

where $\mathbf{E}$ stands for the extended phonon-phason strain field defined as $\mathbf{E} = \{\partial_x u_x, \partial_y u_y, (\partial_x u_y + \partial_y u_x)/2, (\partial_y u_x + \partial_x u_y)/2, \partial_x w_x, \partial_y w_y, \partial_y w_x, \partial_x w_y\}$ and $\tilde{C}$ represents the phonon-phason elastic tensor. Closed formulas for the elements of this tensor as well as for the γ's couplings in terms of the ground state wave function are provided in Supplemental Material [45]; see also Refs. [3,42–44,46] for details of the elastic theory of classical quasicrystals. The presence of the term $\Pi\cdot\nabla\theta$ couples the phonon-phason degrees of freedom with the degrees of freedom corresponding to the overall phase and density of the wave function (see Section II of Supplemental Material [45]). This mechanism leads to a hybridization process which is ultimately responsible for the phenomenology discussed below. The expression in Eq. (3) for the low energy effective action of a bosonic quasicrystal is one of the main results of this work. It allows qualitative and quantitative predictions since all couplings are known in terms of the ground state wave function of the system. Moreover, it generalizes the well-known density-phase action of a homogeneous condensate [40], not only to the present case of quantum quasicrystals but also to supersolids if we eliminate the phasonic degrees of freedom $\mathbf{\Pi}_\perp(\mathbf{x},\tau)$ and $\mathbf{w}(\mathbf{x},\tau)$ and consider that the set $\{G_{\mathbf{n}}\}$ is generated from a two vector basis [39,47–51].

Elementary excitations for the dodecagonal QC—The effective action in Eq. (3) can be recast as $\delta S = \frac{1}{2}\int[d\omega/(2\pi)][d^2q/(2\pi)^2]\hat{\boldsymbol{\eta}}(\mathbf{q},\omega)^\dagger \mathbf{M}(\mathbf{q},\omega)\hat{\boldsymbol{\eta}}(\mathbf{q},\omega)$, where $\hat{\boldsymbol{\eta}}(\mathbf{q},\omega) = [\delta\hat{n}_0(\mathbf{q},\omega), \hat{\theta}(\mathbf{q},\omega), \hat{\Pi}_x(\mathbf{q},\omega), \hat{u}_x(\mathbf{q},\omega), \hat{\Pi}_y(\mathbf{q},\omega), \hat{u}_y(\mathbf{q},\omega), \hat{\Pi}_{x,\perp}(\mathbf{q},\omega), \hat{w}_x(\mathbf{q},\omega), \hat{\Pi}_{y,\perp}(\mathbf{q},\omega), \hat{w}_y(\mathbf{q},\omega)]$, and the energy-momentum dispersion relations $\epsilon(\mathbf{q}) = \omega(\mathbf{q})$ can be computed by solving the equation $\det[\mathbf{M}(\mathbf{q}, i\omega(\mathbf{q}))] = 0$ [40]. The dodecagonal quasicrystal [Fig. 1(a)] is the simplest case due to the absence of the coupling between phonons and phasons. The latter are deformations of the density pattern which are absent in ordinary crystals. We obtain analytical expressions for the dispersion relation of the five gapless modes [45,52,53]. In this case there are three longitudinal modes and two transverse modes, as schematically represented in Fig. 1(b). Two of the longitudinal modes result from the hybridization of the condensate sound mode (corresponding to a modulation of the overall phase θ) with the longitudinal phonon mode, while the transverse phonon as well as the phason mode remain decoupled.

To deepen our understanding of the excitation modes we calculate the eigenvectors $\boldsymbol{\eta}_j(\mathbf{q})$ using the charateristic equation $\mathbf{M}(\mathbf{q}, i\omega_j(\mathbf{q}))\hat{\boldsymbol{\eta}}_j(\mathbf{q}) = \mathbf{0}$ for each excitation mode. Each eigenvector corresponds to a fluctuation field in real space and time given by $\boldsymbol{\eta}_j(\mathbf{x},t) = \mathrm{Re}[\hat{\boldsymbol{\eta}}_j(\mathbf{q}) \exp(i(\mathbf{q}\cdot\mathbf{x} - \omega_j(\mathbf{q})t))]$. By expanding Eq. (2) to linear order in the fluctuation fields we obtain a general expression for the correction to the ground state wave function: $\delta\psi_{j,\mathbf{q}} = [u_{j,\mathbf{q}}(\mathbf{r})\exp(i(\mathbf{q}\cdot\mathbf{r} - \omega_j(\mathbf{q})t)) - v_{j,\mathbf{q}}(\mathbf{r})^*\exp(-i(\mathbf{q}\cdot\mathbf{r} - \omega_j(\mathbf{q})t))]$, allowing us to identify the Bogoliubov modes $u_{j,\mathbf{q}}(\mathbf{r})$ and $v_{j,\mathbf{q}}(\mathbf{r})$ [45]. The local phase and density fluctuations can then be written as $\Delta\rho_{j,\mathbf{q}} = |u_{j,\mathbf{q}}(\mathbf{r}) - v_{j,\mathbf{q}}(\mathbf{r})|^2$ and $\Delta\varphi_{j,\mathbf{q}} = |u_{j,\mathbf{q}}(\mathbf{r}) + v_{j,\mathbf{q}}(\mathbf{r})|^2$ [52,53]. In Fig. 1(c) (1) we show the typical behavior of these quantities. Each column corresponds to a mode in Fig. 1(b) in increasing order of excitations energy. In agreement with previous predictions for supersolids [52], the hybridized longitudinal phonon and condensate modes present nonvanishing $[O(1)]$ phase and density fluctuations in the limit of long wavelength $q \to 0$, while for the transverse phonon mode the fluctuations of density and phase are $O(1)$ and $O(q)$, respectively. On the other hand, while displaying the same scaling properties of the transverse phonon modes, phasons feature density and phase fluctuation patterns that present a different behavior around the center of the quasicrystal structure [54] [compare, e.g., panels (e) and (i) of Fig. 1]. Mathematically, this is ultimately a consequence of the phason's property of producing a redistribution of the QC structure, destroying the center of the quasicrystal without altering the average properties and stability of the system [55]. Finally, we would like to remark that differently from the case of supersolids, here all density and phase fluctuations patterns are aperiodic.

Excitations in decagonal and octagonal QCs—In the case of 10- and 8-fold quasicrystals, the presence of the

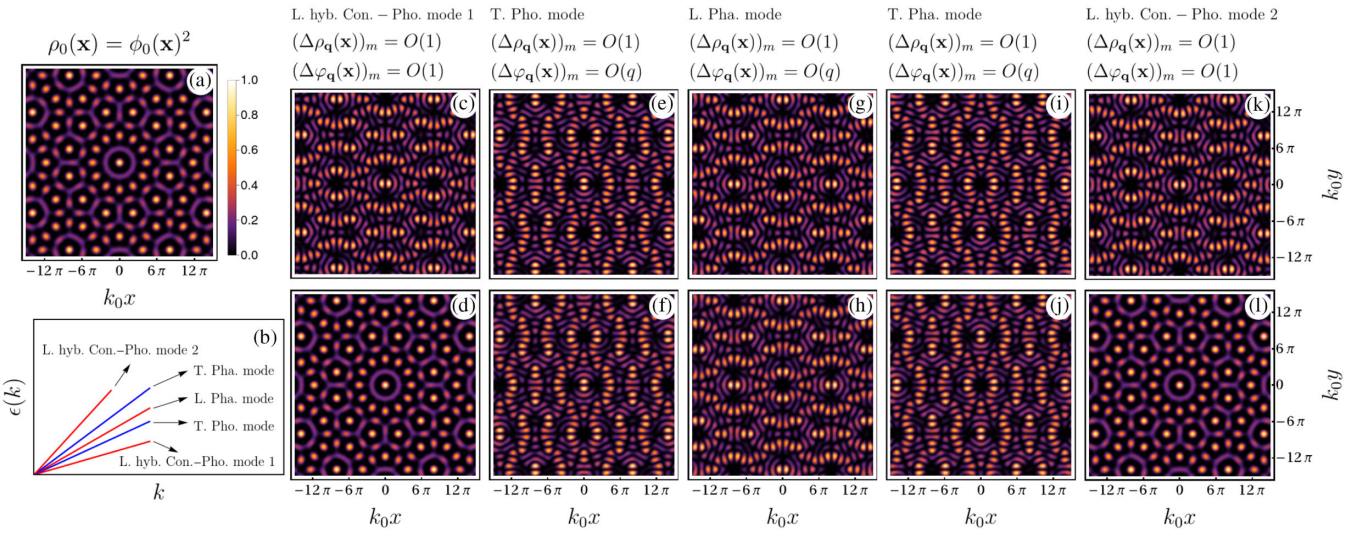

FIG. 1. Typical density pattern (a) and low energy excitations of a dodecagonal QQC in the low momentum regime (b) to (1). The color scale included in (a) applies to all figures provided each profile is normalized by the maximum of the corresponding quantity. (b) Dispersion relation $\epsilon(k)$ for the gapless excitation modes of a dodecagonal QQC, consisting of two longitudinal hybridized condensate-phonon modes [L. hyb. Con.-Phon. mode 1(2)], one transverse phonon mode (T. Pho. mode), and two phason modes, one longitudinal and the other transverse (L. and T. Pha. mode, respectively). (c) to (1) Density fluctuations $\Delta\rho_{\mathbf{q}}(\mathbf{x})$ (first row) and phase fluctuations $\Delta\varphi_{\mathbf{q}}(\mathbf{x})$ (second row) in the low momentum regime for each gapless excitation mode. The density plots are ordered from left to right as they appear in (b), considering an increasing order of the excitation energy. The scaling behavior of the density and phase fluctuations for each mode is given at the top of each column. The momentum of the excitation $\mathbf{q}$ is chosen along the x axis in all cases; see Ref. [45] for detailed information.

phonon-phason coupling leads to a characteristic equation $\det[\mathbf{M}(\mathbf{q}, i\omega(\mathbf{q}))] = 0$ with convoluted analytical solutions. However, some general properties can be obtained from the numerical solution of this problem. In the case of the decagonal quasicrystal, the longitudinal and transverse modes separately hybridize among themselves, leading to two groups of three and two modes, respectively, all with isotropic dispersion relations. In contrast, for the octagonal quasicrystal, the structure of the elasticity action characterized by an anisotropic phason contribution and a finite phonon-phason coupling produces anisotropic dispersion relations $\epsilon(\mathbf{q})$ with propagation speed c_s that depends on the orientation of the momentum $\mathbf{q}$ when $q \to 0$. Additionally, unless the momentum of the excitation $\mathbf{q}$ is oriented along one of the symmetry axes of the quasicrystal, every mode has a longitudinal and a transverse component. As an example, we show in Fig. 2(a) the anisotropic behavior of the propagation speed and hybridization of modes for an octagonal QC. The numerical evaluation was carried out considering values of the couplings for which the system displays strong anisotropy and hybridization effects [45]. Although we have used arbitrary numeric parameters for these calculations, single mode estimates of the full elastic tensor $\tilde{C}$ are possible supporting the projection that the phonon-phason coupling will be of the same order of the phonon-phonon and phason-phason elastic couplings. This justifies the general expectation that the octagonal quasicrystal structure will display significant anisotropic properties. Moreover, we study the longitudinal to transverse character of the excitation modes evaluating the angle $\delta(\mathbf{q}, \mathbf{u})$ between the wave vector of the excitation $\mathbf{q}$ and the direction in which the field $\mathbf{u}$ oscillates as the excitation propagates. In this way, the red to blue color gradient used in Fig. (2) depicts the longitudinal $(\mathbf{u} \| \mathbf{q})$ to transverse $(\mathbf{u} \perp \mathbf{q})$ feature of the excitations.

Interestingly, the propagation of excitations along nonequivalent symmetry axes of the octagonal quasicrystal produces an exchange of the longitudinal and transverse character for some modes. Moreover, the evaluation of the local density and phase fluctuations profile in this case shows that the scaling of the fluctuations when the propagation direction of the excitation does not coincide with a symmetry axes of the quasicrystal are all $O(1)$. Meanwhile, in the opposite case, longitudinal modes have density and phase fluctuations of amplitude $O(1)$ and transverse modes with density fluctuations $O(1)$ and phase fluctuations $O(q)$. The aperiodic patterns of phase and density fluctuations for each scenario discussed can be found in [45].

Instabilities of the quantum quasicrystal phase—The study of instabilities in general sheds light on the occurrence of phase transitions in the system. In our case, we expect a transition to a homogeneous state at low ρU values; meanwhile, at high ρU the loss of phase coherence over the system signals in principle a transition to a classical quasicrystal state. A first analysis of the instabilities can be based on the behavior of the propagation speed of the gapless modes. With this aim we consider the case of the decagonal QC structure and pursue the calculation of the couplings in the action (3), considering small amplitudes of the QC modulation [45]. In order to make a numerical evaluation possible without defining a particular form of the interaction potential, we assume that the QC amplitude is a concave increasing function of ρU [56]. Although this is the expected behavior of this quantity, such ansatz does not intend to capture the actual quantitative behavior of a certain model [45]. The results of the isotropic propagation speed of each mode for the decagonal quasicrystal are shown in Fig. 2(b) as a function of ρU. One recognizes a discontinuous behavior of the propagation speed at the homogeneous-superfluid-to-quantum-quasicrystal phase transition, analogous to

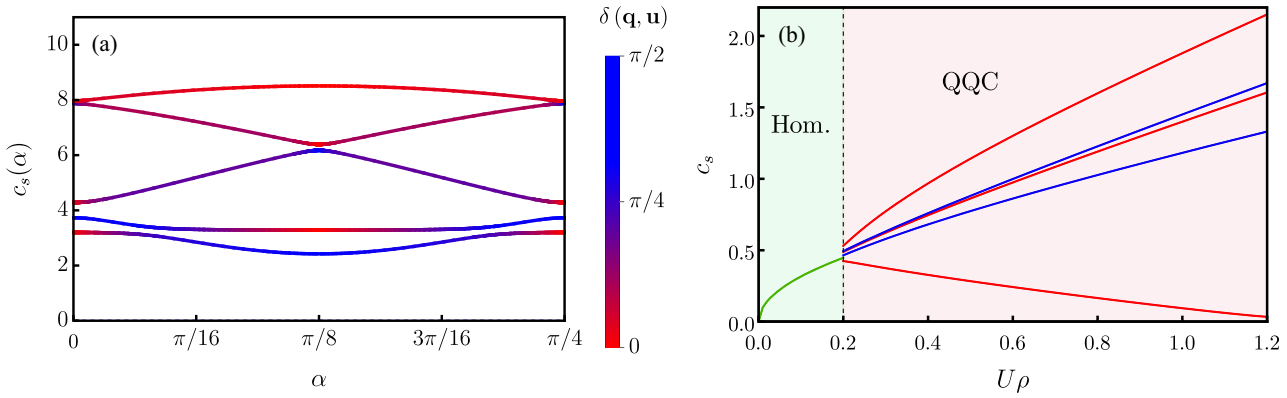

FIG. 2. Typical behavior of the propagation speed of the gapless modes (a) as a function of the orientation α of the momentum of the excitation $\mathbf{q}$ in an octagonal QQC, and (b) as a function of $U\rho$ for a decagonal QQC in a region containing the transition to the homogeneous superfluid phase (Hom.). The red to blue gradient of color is used to indicate the longitudinal to transverse character of a given excitation mode using the angle $[\delta(\mathbf{q}, \mathbf{u})]$ of the field $\mathbf{u}$ respect to $\mathbf{q}$ as a measure of this property.

previous predictions in supersolids [39,47,52,57], and a continuous behavior at the quantum-to-classical-quasicrystal transition at high enough densities where the propagation speed of the lowest mode vanishes [58,59]. As we shall see next, this transition corresponds to the breaking of quantum phase coherence.

To further explore the nature of the instabilities we compute the second-order correlations of the fluctuation fields. At the lower density boundary, when the QC amplitude is small and the ground state wave function is dominated by the main Fourier amplitude of the pattern (c_1), we find that Z, $Z_\perp$, and all elastic couplings in $\tilde{C}$ approaches zero as c_1^2, while γ and $\gamma_\perp$ diverges as c_1^{-2}. This behavior leads us to the conclusion that in this regime $\langle \delta n_0^2 \rangle$ and $\langle \theta^2 \rangle$ remain finite, while $\langle \mathbf{\Pi}^2 \rangle \propto c_1^2$, $\langle \mathbf{\Pi}_\perp^2 \rangle \propto c_1^2$, $\langle \mathbf{u}^2 \rangle \propto c_1^{-2}$, and $\langle \mathbf{w}^2 \rangle \propto c_1^{-2}$, as $c_1 \to 0$, with $c_1 \gg c_{n>1}$ [45]. In this scenario the average wave function can be roughly approximated as $\langle \phi(x,\tau) \rangle \approx \sqrt{\rho} \sum_{\mathbf{n}} c_{\mathbf{n}} \exp(i\mathbf{G}_{\mathbf{n}} \cdot \mathbf{x}) \exp(-G_{\mathbf{n}}^2 \langle \mathbf{u}^2 \rangle/4 - G_{\mathbf{n},\perp}^2 \langle \mathbf{w}^2 \rangle/4 - \langle \theta^2 \rangle/2)$. This result confirms that close enough to the superfluid-quantum-quasicrystal stability boundary, where we have large phonon and phason fluctuations, there is a strong nonperturbative "renormalization" of the Fourier amplitudes of the quasicrystal profile [60]. This phenomenology suggests that in cases in which the mean field superfluid to quantum quasicrystal phase transition is weak enough, the nature of the transition could be modified to a continuous one, where phonon and phason fluctuations promote the creation of topological defects (dislocations) leading eventually to the stabilization of an intermediate topological phase, analogous to the hexatic phase between the solid and the liquid in the two-step thermal melting process of certain two-dimensional solids [61,62].

At the upper boundary of the quantum quasicrystal phase ($\gamma\rho \to 1^+$) all couplings of the effective action in Eq. (3) remain finite; however, in this limit the propagation speed of the lower hybridized mode approaches zero, as observed before. This behavior signals the disappearance of this mode, in the same way in which the lower energy excitation mode disappears at the supersolid to normal solid phase transition [58]. Calculating the correlations of the fluctuation fields in this regime, we obtain to leading order that $\langle \delta n_0^2 \rangle$ $\langle \mathbf{u}^2 \rangle, \langle \mathbf{w}^2 \rangle$, and $\langle \mathbf{\Pi}_\perp^2 \rangle$ remain finite as the stability boundary is approached, while $\langle \theta^2 \rangle \propto (\gamma\rho - 1)^{-1/2}$ and $\langle \mathbf{\Pi}^2 \rangle \propto (\gamma\rho - 1)^{-1/2}$ [45]. This result is to be expected since in the high ρU regime the localization of particles should eventually lead the system to the loss of quantum phase coherence. Interestingly, due to the effective $\mathbf{\Pi} \cdot \nabla\theta$ interaction the destabilization of the $\theta(\mathbf{x},\tau)$ field also produces the destabilization of the $\mathbf{\Pi}(\mathbf{x},\tau)$ field, indicating the natural breakdown of our theory at this phase boundary. All evidence available in this case indicates a second order phase transition in this limit, as predicted in supersolid systems [39,52,63,64].

Conclusions—We have developed the elastic theory of a self-organized quantum quasicrystal with 8-, 10-, or 12-fold rotational symmetry. We obtained the effective action of the system described in terms of the global wave function phase, the two-dimensional phonon and phason fields, and their respective conjugate density fields. From here, we were able to prove from first principles the existence of five gapless extended low energy excitation modes [65] for the considered two-dimensional QC structures [37,38]. We showed that the presence of the $\mathbf{\Pi} \cdot \nabla\theta$ coupling in our effective theory produces the hybridization of the condensate sound mode with phonon and phason modes, leading to a rich phenomenology depending on the QC structure. A particularly interesting finding was that, due to the phonon-phason coupling, the octagonal QC structure develops an anisotropic speed of sound that depends on direction of the propagation, as well as that all modes show a mixed longitudinal-transverse character. Finally, our results shed light on the behavior of the low energy fluctuation fields at the thermodynamic boundaries of the quantum quasicrystal phase, elucidating possible scenarios for phase transitions in two dimensions. Our results are directly relevant for experimental platforms involving ultracold atomic gases. An important future extension will be the applicaton to TBG, which requires including new elements like the intra- vs interlayer, as well as the lattice-electron coupling [27].

Acknowledgments—A. M. C. acknowledge Max Planck Institute for the Physics of Complex Systems (MPIPKS) for financial support and hospitality.

[1] C. Janot, *Quasicrystals, A Primer* (Oxford University Press, New York, 1997).
[2] D. Shechtman, I. Blech, D. Gratias, and J. W. Cahn, Metallic phase with long-range orientational order and no translational symmetry, Phys. Rev. Lett. **53**, 1951 (1984).
[3] D. Levine and P. J. Steinhardt, Quasicrystals: A new class of ordered structures, Phys. Rev. Lett. **53**, 2477 (1984).
[4] A. P. Tsai, Icosahedral clusters, icosaheral order and stability of quasicrystals–a view of metallurgy, Sci. Technol. Adv. Mater. **9**, 013008 (2008).
[5] L. Bindi, P. J. Steinhardt, N. Yao, and P. J. Lu, Natural quasicrystals, Science **324**, 1306 (2009).
[6] R. Lifshitz and D. M. Petrich, Theoretical model for Faraday waves with multiple-frequency forcing, Phys. Rev. Lett. **79**, 1261 (1997).
[7] B. Freedman, R. Lifshitz, J. W. Fleischer, and M. Segev, Phason dynamics in nonlinear photonic quasicrystals, Nat. Mater. **6**, 776 (2007).
[8] K. Barkan, H. Diamant, and R. Lifshitz, Stability of quasicrystals composed of soft isotropic particles, Phys. Rev. B **83**, 172201 (2011).
[9] E. Sagi and Z. Nussinov, Emergent quasicrystals in strongly correlated systems, Phys. Rev. B **94**, 035131 (2016).
[10] M. Zu, P. Tan, and N. Xu, Forming quasicrystals by monodisperse soft core particles, Nat. Commun. **8**, 2089 (2017).

[11] K. Barkan, M. Engel, and R. Lifshitz, Controlled self-assembly of periodic and aperiodic cluster crystals, Phys. Rev. Lett. **113**, 098304 (2014).
[12] G. Pupillo, P. c. v. Ziherl, and F. Cinti, Quantum cluster quasicrystals, Phys. Rev. B **101**, 134522 (2020).
[13] B. R. de Abreu, F. Cinti, and T. Macrì, Superstripes and quasicrystals in bosonic systems with hard-soft corona interactions, Phys. Rev. B **105**, 094505 (2022).
[14] A. Mendoza-Coto, R. Turcati, V. Zampronio, R. Díaz-Méndez, T. Macrì, and F. Cinti, Exploring quantum quasicrystal patterns: A variational study, Phys. Rev. B **105**, 134521 (2022).
[15] S. Gopalakrishnan, I. Martin, and E. A. Demler, Quantum quasicrystals of spin-orbit-coupled dipolar bosons, Phys. Rev. Lett. **111**, 185304 (2013).
[16] F. Mivehvar, H. Ritsch, and F. Piazza, Emergent quasicrystalline symmetry in light-induced quantum phase transitions, Phys. Rev. Lett. **123**, 210604 (2019).
[17] M. Grossklags, M. Ciardi, V. Zampronio, F. Cinti, and A. Mendoza-Coto, Self-induced Bose glass phase in quantum quasicrystals, Results Phys. **65**, 107991 (2024).
[18] M. Ciardi, A. Angelone, F. Mezzacapo, and F. Cinti, Quasicrystalline Bose glass in the absence of disorder and quasidisorder, Phys. Rev. Lett. **131**, 173402 (2023).
[19] R. Gautier, H. Yao, and L. Sanchez-Palencia, Strongly interacting bosons in a two-dimensional quasicrystal lattice, Phys. Rev. Lett. **126**, 110401 (2021).
[20] Z. Zhu, H. Yao, and L. Sanchez-Palencia, Thermodynamic phase diagram of two-dimensional bosons in a quasicrystal potential, Phys. Rev. Lett. **130**, 220402 (2023).
[21] K. Viebahn, M. Sbroscia, E. Carter, J.-C. Yu, and U. Schneider, Matter-wave diffraction from a quasicrystalline optical lattice, Phys. Rev. Lett. **122**, 110404 (2019).
[22] M. Sbroscia, K. Viebahn, E. Carter, J.-C. Yu, A. Gaunt, and U. Schneider, Observing localization in a 2D quasicrystalline optical lattice, Phys. Rev. Lett. **125**, 200604 (2020).
[23] J.-C. Yu, S. Bhave, L. Reeve, B. Song, and U. Schneider, Observing the two-dimensional Bose glass in an optical quasicrystal, Nature (London) **633**, 338 (2024).
[24] T. D. Farokh Mivehvar, Francesco Piazza, and H. Ritsch, Cavity QED with quantum gases: New paradigms in many-body physics, Adv. Phys. **70**, 1 (2021).
[25] M. Bonifacio, F. Piazza, and T. Donner, Laser-painted cavity-mediated interactions in a quantum gas, PRX Quantum **5**, 040332 (2024).
[26] W. Yao, E. Wang, C. Bao, Y. Zhang, K. Zhang, K. Bao, C. K. Chan, C. Chen, J. Avila, M. C. Asensio, J. Zhu, and S. Zhou, Quasicrystalline 30° twisted bilayer graphene as an incommensurate superlattice with strong interlayer coupling, Proc. Natl. Acad. Sci. U.S.A. **115**, 6928 (2018).
[27] H. Ochoa, Moiré-pattern fluctuations and electron-phason coupling in twisted bilayer graphene, Phys. Rev. B **100**, 155426 (2019).
[28] C. Burgess, Goldstone and pseudo-Goldstone bosons in nuclear, particle and condensed-matter physics, Phys. Rep. **330**, 193 (2000).
[29] D. G. Barci, A. Mendoza-Coto, and D. A. Stariolo, Nematic phase in stripe-forming systems within the self-consistent screening approximation, Phys. Rev. E **88**, 062140 (2013).
[30] A. Mendoza-Coto, D. A. Stariolo, and L. Nicolao, Nature of long-range order in stripe-forming systems with long-range repulsive interactions, Phys. Rev. Lett. **114**, 116101 (2015).
[31] A. Mendoza-Coto, D. E. B. de Oliveira, L. Nicolao, and R. Díaz-Méndez, Topological phase diagrams of the frustrated Ising ferromagnet, Phys. Rev. B **101**, 174438 (2020).
[32] P. Surówka, Dual gauge theory formulation of planar quasicrystal elasticity and fractons, Phys. Rev. B **103**, L201119 (2021).
[33] L. Radzihovsky, A. Kuklov, N. Prokof'ev, and B. Svistunov, Superfluid edge dislocation: Transverse quantum fluid, Phys. Rev. Lett. **131**, 196001 (2023).
[34] A. Kuklov, N. Prokof'ev, L. Radzihovsky, and B. Svistunov, Transverse quantum fluids, Phys. Rev. B **109**, L100502 (2024).
[35] A. Gromov and L. Radzihovsky, Colloquium: Fracton matter, Rev. Mod. Phys. **96**, 011001 (2024).
[36] A. Mendoza-Coto, V. Mattiello, R. Cenci, N. Defenu, and L. Nicolao, Melting of the two-dimensional solid phase in the Gaussian core model, Phys. Rev. B **109**, 064101 (2024).
[37] R. Lifshitz, Comment on quantum quasicrystals of spin-orbit-coupled dipolar bosons, Phys. Rev. Lett. **113**, 079602 (2014).
[38] M. Sandbrink, J. Roth, and M. Schmiedeberg, Comment on quantum quasicrystals of spin-orbit-coupled dipolar bosons, Phys. Rev. Lett. **113**, 079601 (2014).
[39] V. Heinonen, K. J. Burns, and J. Dunkel, Quantum hydrodynamics for supersolid crystals and quasicrystals, Phys. Rev. A **99**, 063621 (2019).
[40] H. T. C. Stoof, D. B. M. Dickerscheid, and K. Gubbels, *Ultracold Quantum Fields*, 1st ed. (Springer, New York, 2009).
[41] M. Pretko and L. Radzihovsky, Symmetry-enriched fracton phases from supersolid duality, Phys. Rev. Lett. **121**, 235301 (2018).
[42] D. Levine, T. C. Lubensky, S. Ostlund, S. Ramaswamy, P. J. Steinhardt, and J. Toner, Elasticity and dislocations in pentagonal and icosahedral quasicrystals, Phys. Rev. Lett. **54**, 1520 (1985).
[43] J. E. S. Socolar, Simple octagonal and dodecagonal quasicrystals, Phys. Rev. B **39**, 10519 (1989).
[44] D.-h. Ding, W. Yang, C. Hu, and R. Wang, Generalized elasticity theory of quasicrystals, Phys. Rev. B **48**, 7003 (1993).
[45] See Supplemental Material at http://link.aps.org/supplemental/10.1103/PhysRevLett.134.136003 for low energy excitations in bosonic quantum quasicrystals.
[46] T.-Y. Fan, *Mathematical Theory of Elasticity of Quasicrystals and Its Applications* (Springer, Singapore, 2016).
[47] M. Kunimi and Y. Kato, Mean-field and stability analyses of two-dimensional flowing soft-core bosons modeling a supersolid, Phys. Rev. B **86**, 060510(R) (2012).
[48] J. Ye, Elementary excitation in a supersolid, Europhys. Lett. **82**, 16001 (2008).
[49] Y. Pomeau and S. Rica, Dynamics of a model of supersolid, Phys. Rev. Lett. **72**, 2426 (1994).
[50] C. Josserand, Y. Pomeau, and S. Rica, Coexistence of ordinary elasticity and superfluidity in a model of a defect-free supersolid, Phys. Rev. Lett. **98**, 195301 (2007).

[51] C. Josserand, Y. Pomeau, and S. Rica, Patterns and supersolids, Eur. Phys. J. Spec. Top. **146**, 47 (2007).
[52] T. Macrì, F. Maucher, F. Cinti, and T. Pohl, Elementary excitations of ultracold soft-core bosons across the superfluid-supersolid phase transition, Phys. Rev. A **87**, 061602(R) (2013).
[53] W.-C. Wu and A. Griffin, Quantized hydrodynamic model and the dynamic structure factor for a trapped Bose gas, Phys. Rev. A **54**, 4204 (1996).
[54] The center of the quasicrystal here is being understood as the special point where all reflections symmetry planes of the quasicrystal pattern intersect. Given the form of our ansatz for $\phi_0(\mathbf{x})$ it coincides with the origin of our coordinates system.
[55] R. Lifshitz, Symmetry breaking and order in the age of quasicrystals, Isr. J. Chem. **51**, 1156 (2011).
[56] Mathematically this means $[\partial c_1(U\rho)/\partial(U\rho)] > 0$ and $[\partial^2 c_1(U\rho)/\partial(U\rho)^2] < 0$, where $c_1(U\rho)$ stands for the modulation amplitude of ϕ_0.
[57] P. B. Blakie, L. Chomaz, D. Baillie, and F. Ferlaino, Compressibility and speeds of sound across the superfluid-to-supersolid phase transition of an elongated dipolar gas, Phys. Rev. Res. **5**, 033161 (2023).
[58] S. Saccani, S. Moroni, and M. Boninsegni, Excitation spectrum of a supersolid, Phys. Rev. Lett. **108**, 175301 (2012).
[59] Although Mean Field treatments of our action consistent with the Gross-Pitaevskki description are not able to reach a strictly zero propagation speed for the lowest mode, beyond Mean Field descriptions have succeeded in observing rigorously the supersolid to normal solid transition [58].
[60] The strong renormalization process is signaled by the non-analytic behavior of $\langle\phi\rangle$ in the limit $c_1 \to 0$ upon inclusion of phonon and phason fluctuations.
[61] D. R. Nelson and B. I. Halperin, Dislocation-mediated melting in two dimensions, Phys. Rev. B **19**, 2457 (1979).
[62] S. Prestipino, F. Saija, and P. V. Giaquinta, Hexatic phase in the two-dimensional Gaussian-core model, Phys. Rev. Lett. **106**, 235701 (2011).
[63] F. Cinti, M. Boninsegni, and T. Pohl, Exchange-induced crystallization of soft-core bosons, New J. Phys. **16**, 033038 (2014).
[64] F. Cinti, A. Cappellaro, L. Salasnich, and T. Macrì, Superfluid filaments of dipolar bosons in free space, Phys. Rev. Lett. **119**, 215302 (2017).
[65] It is worth to mention, that due to the lack of periodicity quantum quasicrystals can also host particle-hole localized excitations with an energy arbitrarily close to zero. See Refs. [66,67].
[66] B. Svistunov, E. Babaev, and N. Prokof'ev, *Superfluid States of Matter* (Taylor & Francis, London, 2015).
[67] Z. Zhu, S. Yu, D. Johnstone, and L. Sanchez-Palencia, Localization and spectral structure in two-dimensional quasicrystal potentials, Phys. Rev. A **109**, 013314 (2024).